



OPEN

Humanized *GPRC6A*^{KGKY} is a gain-of-function polymorphism in mice

Min Pi¹✉, Fuyi Xu², Ruisong Ye¹, Satoru K. Nishimoto³, Robert A. Kesterson⁴, Robert W. Williams², Lu Lu² & L. Darryl Quarles¹✉

GPRC6A is proposed to regulate energy metabolism in mice, but in humans a KGKY polymorphism in the third intracellular loop (ICL3) is proposed to result in intracellular retention and loss-of-function. To test physiological importance of this human polymorphism *in vivo*, we performed targeted genomic humanization of mice by using CRISPR/Cas9 (clustered regularly interspaced short palindromic repeats-CRISPR associated protein 9) system to replace the RKLP sequence in the ICL3 of the *GPRC6A* mouse gene with the uniquely human KGKY sequence to create *Gprc6a*^{KGKY-knockin} mice. Knock-in of a human KGKY sequence resulted in a reduction in basal blood glucose levels and increased circulating serum insulin and FGF-21 concentrations. *Gprc6a*^{KGKY-knockin} mice demonstrated improved glucose tolerance, despite impaired insulin sensitivity and enhanced pyruvate-mediated gluconeogenesis. Liver transcriptome analysis of *Gprc6a*^{KGKY-knockin} mice identified alterations in glucose, glycogen and fat metabolism pathways. Thus, the uniquely human *GPRC6A*^{KGKY} variant appears to be a gain-of-function polymorphism that positively regulates energy metabolism in mice.

GPRC6A is a family C G-protein coupled receptor (GPCR) that is reported to be capable of sensing multiple ligands. There is a consensus that *GPRC6A* is activated by basic amino acid, including L-arginine, L-ornithine, and L-lysine^{1–3}. Several laboratories have shown that *GPRC6A* is activated by the bone-derived peptide, osteocalcin (Ocn)^{4–10}, and testosterone (T)^{1,11–13}, and natural products in green tea¹⁴. In contrast, other investigators have failed to show that either testosterone or Ocn activates *GPRC6A*^{15,16}. *GPRC6A* is expressed in several tissues, including β -cells, liver hepatocytes, skeletal muscle, fat, and Leydig cells where it is reported to regulate glucose and fat metabolism and hormone production.

Gprc6a^{-/-} mice exhibit complex metabolic derangements that resemble metabolic syndrome (MetS), including glucose intolerance, insulin resistance, and fatty liver^{1,9,17–20}. Conditional deletion of *Gprc6a* in Leydig cells attenuates Ocn induced T production by the testes²¹, in pancreatic β -cells regulates insulin secretion^{9,19}, and in skeletal muscle regulates muscle glucose and fatty acid utilization and IL-6 production independent of insulin during exercise^{20,22,23}. The similar phenotypes of *Gprc6a*^{-/-} and *Ocn*^{-/-} mice and the additive phenotypic effects in compound *Gprc6a*^{+/-}/*Ocn*^{+/-} mice support the physiological importance of Ocn as the cognate *GPRC6A* ligand²⁴. The *GPRC6A* endocrine network appears to be strongly influenced by genetic, sex-dependent and environmental factors, since the phenotype of Ocn and *GPRC6A* deficiencies are variable^{3,15,16,24–28}.

The clinical significance of *GPRC6A* in regulating energy metabolism in humans remains to be established. The ancestral RKLP polymorphism in the 3rd intracellular loop found in mice and all other species is a minor variant in humans, most commonly found in African Americans (40%)^{15,16,28,29}. Rather a *GPRC6A*^{KGKY} variant, which replaces the RKLP sequence in the 3rd intracellular loop with the KGKY insertion/deletion, evolved uniquely in humans^{25,30} and is present in 91% of Europeans, and 99% of Asians, but only 60% of people of African descent. While the ancestral *GPRC6A*^{RKLP} variant is located on the cell surface and undergoes ligand-dependent recycling like classical G-protein coupled receptors, the newly evolved *GPRC6A*^{KGKY} variant is predominantly

¹Department of Medicine, University of Tennessee Health Science Center, 19 S Manassas St., Memphis, TN 38163, USA. ²Department of Genetics, Genomics and Informatics, University of Tennessee Health Science Center, 19 S Manassas St., Memphis, TN 38163, USA. ³Department of Microbiology, Immunology and Biochemistry, University of Tennessee Health Science Center, 19 S Manassas St., Memphis, TN 38163, USA. ⁴Department of Genetics, University of Alabama at Birmingham, 720 20th Street South, Birmingham, AL 35294, USA. ✉email: mpi@uthsc.edu; dquarles@uthsc.edu

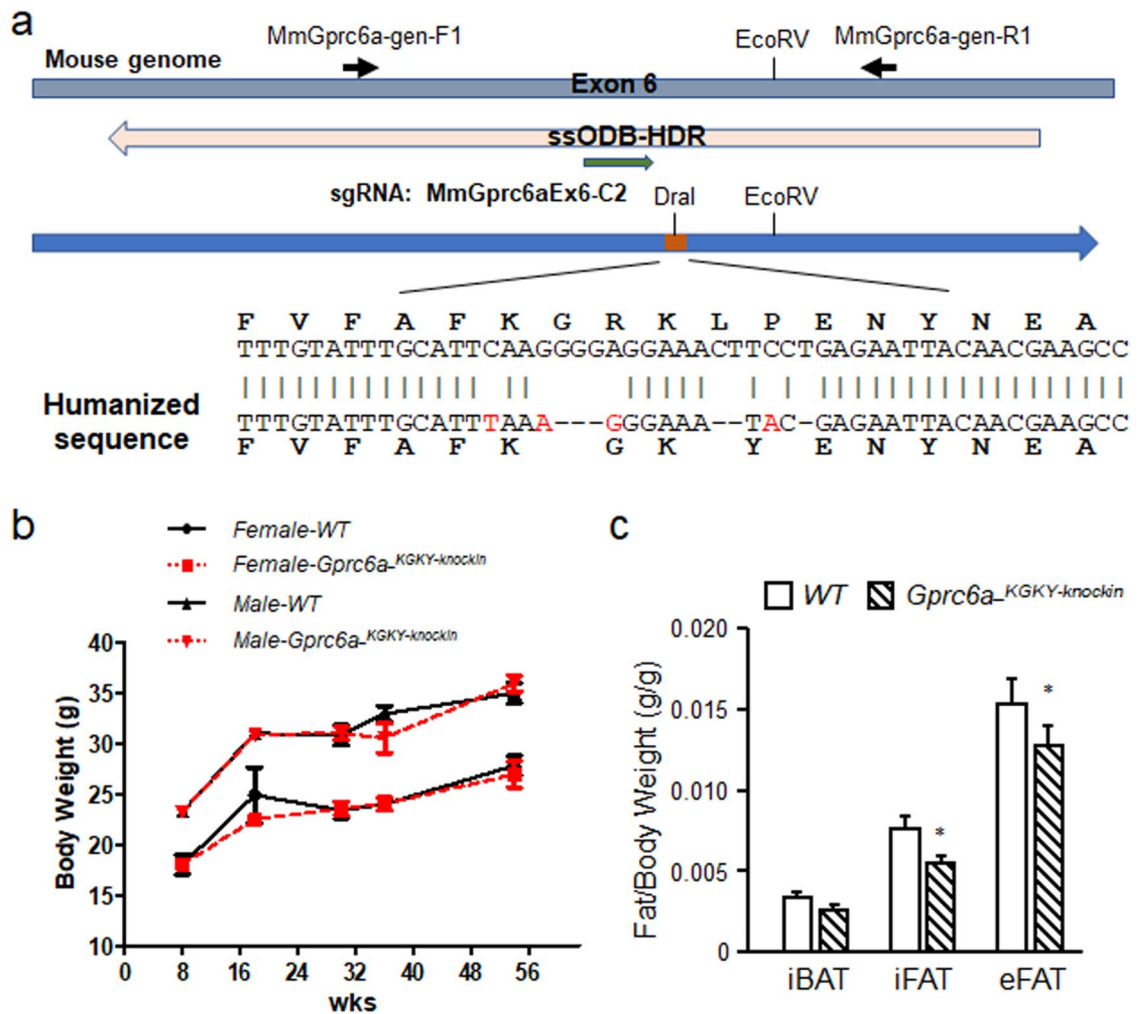


Figure 1. Creation of *Gprc6a*^{KGKY-knockin} mice. (a) Structure of *Gprc6a* exon 6, knockin sequence and genotype primers and *Dra* I restricted enzyme location. The orange box shows the KY location in blue arrow. The yellow arrow shows the ssODB-HDR location. The green arrow shows sgRNA location. (b) Comparison of the body weight in wild type and *Gprc6a*^{KGKY-knockin} mice at age from 8 to 54 weeks. (c) Site specific brown and white fat content in 20 week-old male mice. Interscapular brown fat (iBAT) and white inguinal fat (iFAT) and epididymal fat (eFAT). Values represent the mean \pm SEM. *Significant difference between wild type mouse *Gprc6a*^{RKLP} and *Gprc6a*^{KGKY-knockin} mice ($P < 0.05$, Student's *t* test; $n = 6$).

located intracellularly in the early endosomes^{13,26}. The *GPRC6A*^{KGKY} variant is inconsistently reported to be either a loss-of-function^{26,31}, or a gain-of-function polymorphism^{13,32} using in vitro cell culture model systems.

To understand the function of this uniquely human KGKY polymorphism in vivo, we have knocked-in the KGKY sequence to replace the ancestral RKLP sequence in the 3rd intracellular loop of the mouse gene. The transgenic mouse model establishes the KGKY insertion/deletion as a gain-of-function polymorphism in vivo.

Results

“Humanized” *Gprc6a*^{KGKY-knockin} transgenic mice have enhanced metabolic functions. Our previous data found that the insertion of the KGKY sequence in the mouse GPRC6A (i.e., humanized mouse GPRC6A^{ICL3_KGKY}) acquires characteristics of the human GPRC6A^{ICL3_KGKY}, namely predominate location to endosome-like intracellular punctuate structures and gain-of-function of mTOR signaling, an evolutionarily conserved pathway in endosomal nutrient signaling^{13,32}. We extend these data, by showing that osteocalcin induces an increase in the magnitude and duration of mTOR signaling in cells transfected with the mGPRC6A^{ICL3_KGKY} mutant compared to the wild-type mouse GPRC6A^{ICL3_RKLP} cDNA in vitro (Figure S1A). In contrast, activation of ERK signaling by osteocalcin was not different between transfected mGPRC6A^{ICL3_KGKY} mutant compared to the wild-type GPRC6A^{ICL3_RKLP} (Figure S1B).

To test the function of this insertion/deletion in vivo, we “humanized” the mouse *Gprc6a* gene by using CRISPR/Cas9 system to replace the ICL3_RKLP sequence in the mouse with the ICL3_KGKY sequence (Fig. 1a). *Gprc6a*^{KGKY-knockin} mice had similar body weights as *Gprc6a*^{RKLP} wild type controls (Fig. 1b). *Gprc6a*^{KGKY-knockin}

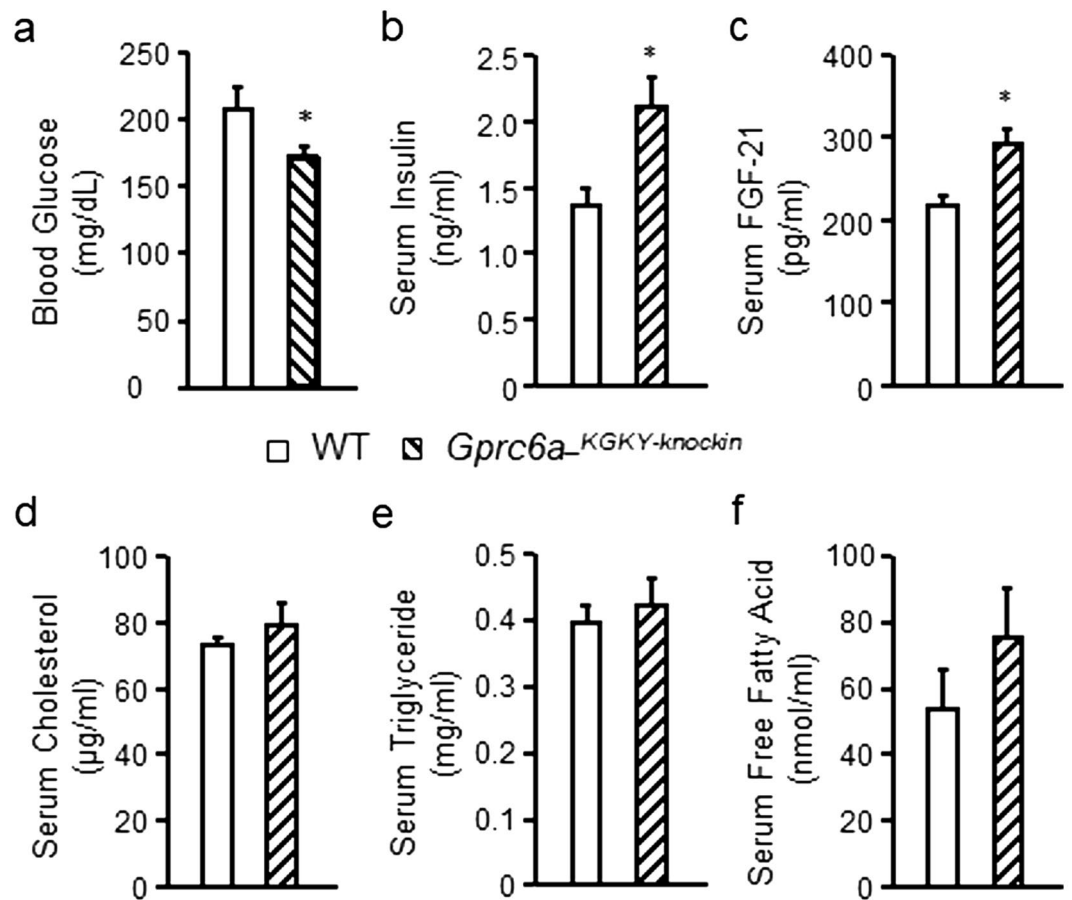


Figure 2. Characterization of *Gprc6a*^{-KGKY-knockin} mice. Comparison of the fasting blood glucose (a), serum insulin (b) and serum FGF-21 levels (c), serum levels of cholesterol (d), triglyceride (e) and free fatty acid (f) in wild type and *Gprc6a*^{-KGKY-knockin} male mice at age of 10 week-old. Values represent the mean \pm SEM. *Significant difference between wild type and *Gprc6a*^{-KGKY-knockin} mice ($P < 0.05$, Student's *t* test; $n = 6$).

male mice had significantly lower inguinal and epididymal white fat mass, but no change in intrascapular brown fat in 20 week-old of age (Fig. 1c).

Gprc6a^{-KGKY-knockin} mice had significantly lower fasting blood glucose concentrations ($P \leq 0.05$, Fig. 2a) and a significant increase in basal serum insulin levels ($P < 0.05$; Fig. 2b). *Gprc6a*^{-KGKY-knockin} mice also exhibited significantly increased serum FGF-21 levels ($P < 0.05$, Fig. 2c). We found no significant changes in serum cholesterol, triglycerides or free fatty acid concentrations in the serum of *Gprc6a*^{-KGKY-knockin} mice compared to controls (Fig. 2d–f).

Gprc6a^{-KGKY-knockin} mice also had an improved glucose tolerance test (GTT) as shown by lower blood glucose concentrations compared to controls at different time points after glucose injection (Fig. 3a). Accordingly, the net area under the curve, which represents the variation in glucose concentration from baseline over the test duration, was smaller in *Gprc6a*^{-KGKY-knockin} mice.

Gprc6a^{-KGKY-knockin} mice lowered blood glucose in response to insulin, but they maintained a higher blood glucose compared to controls throughout most of the insulin tolerance test³³ (Fig. 3b). The pyruvate tolerance test (PTT) assesses the effects of glucose production through gluconeogenesis. *Gprc6a*^{-KGKY-knockin} mice had a greater increase in blood glucose in response to pyruvate (Fig. 3c) compared to wild-type (*Gprc6a*^{-RKL^P}) mice, consistent with higher gluconeogenesis in *Gprc6a*^{-KGKY-knockin} mice.

Next, we compared the serum insulin and FGF-21 response in *Gprc6a*^{-KGKY-knockin} mice with the pharmacological effects of GPRC6A activation by its ligand Ocn. We found that Ocn administration resulted in increases in both insulin and FGF-21 circulating levels (Fig. 4a, b). In addition, Ocn stimulated FGF-21 message levels in the liver (Fig. 4c).

Since FGF-21 is produced by the liver, we next examined additional hepatic parameters in *Gprc6a*^{-KGKY-knockin} mice. We found slight reductions in liver cholesterol content but no differences in liver triglyceride or glycogen content in *Gprc6a*^{-KGKY-knockin} mice (Fig. 5a–c). Liver glucose-6-P levels were significantly elevated in *Gprc6a*^{-KGKY-knockin} mice compared to wild-type mice (Fig. 5d), consistent with GPRC6A regulating glucose metabolism in the liver.

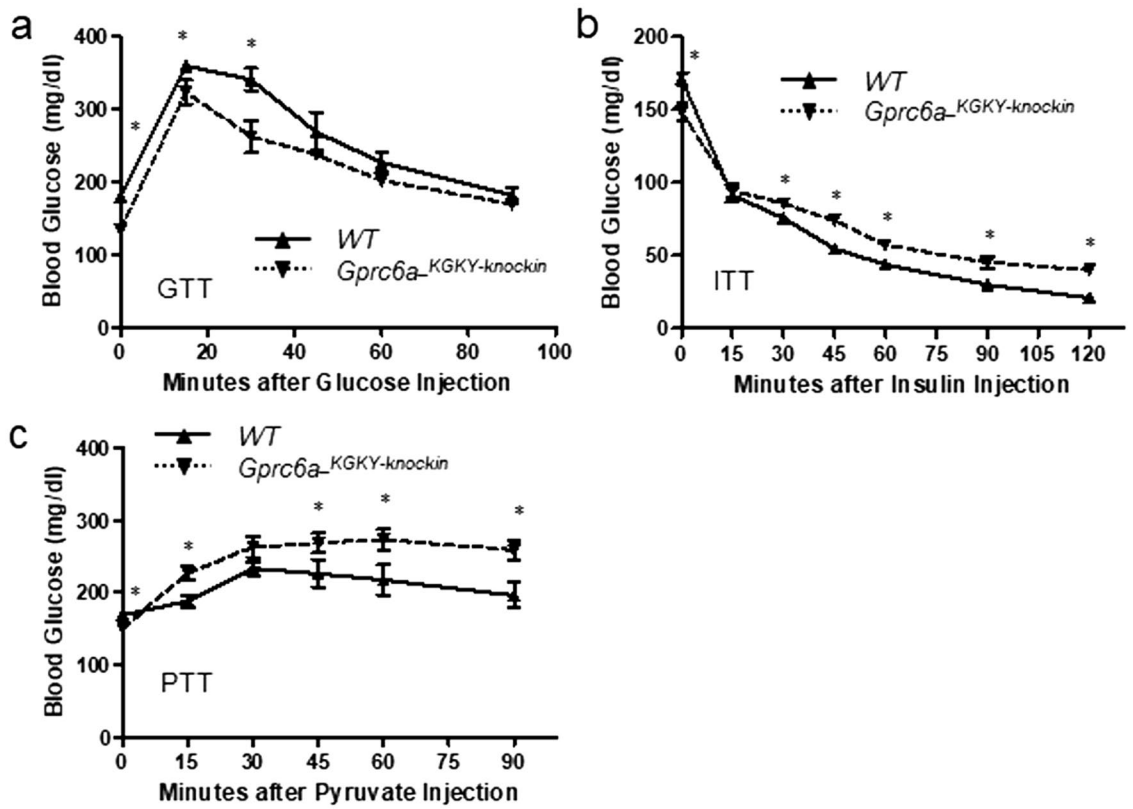


Figure 3. Tolerance tests in *Gprc6a*^{-KGKY-knockin} mice. Blood glucose (mg/ml) during GTT (a), ITT (b) and PTT (c) in 10-week-old wild type and *Gprc6a*^{-KGKY-knockin} mice. Data represent the mean ± SEM from more than 5 male mice in each group. *Difference from wild type and *Gprc6a*^{-KGKY-knockin} mice at $P < 0.05$, two-way ANOVA with Tukey's multiple comparisons test.

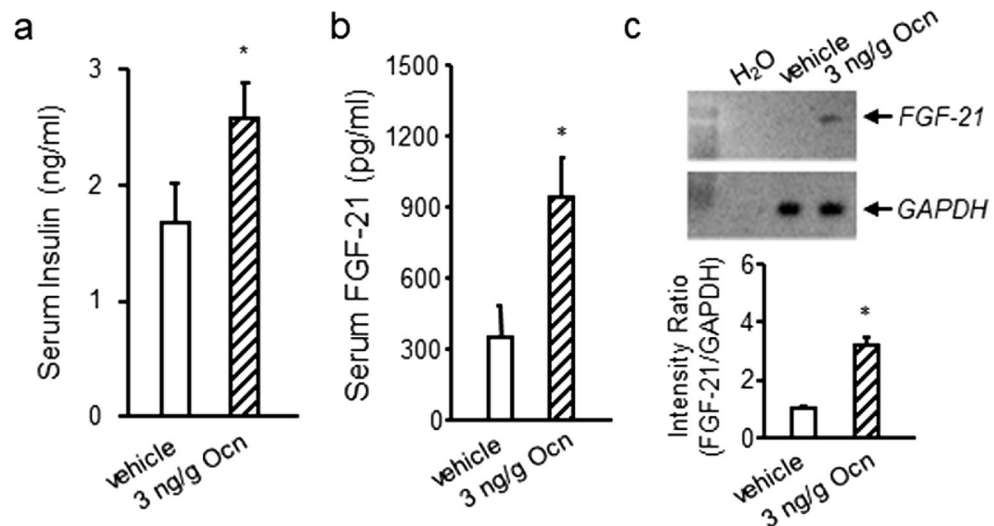


Figure 4. Effects of Ocn administration on insulin and FGF-21 in wild-type mice. Effect of Ocn administration to increase serum insulin (a) and FGF-21 (b) concentrations and liver message levels (c) in wild-type male mice. Values represent the mean ± SEM. *Significant difference between control group and Ocn-treated mice ($P < 0.05$, Student's *t* test; $n = 5$).

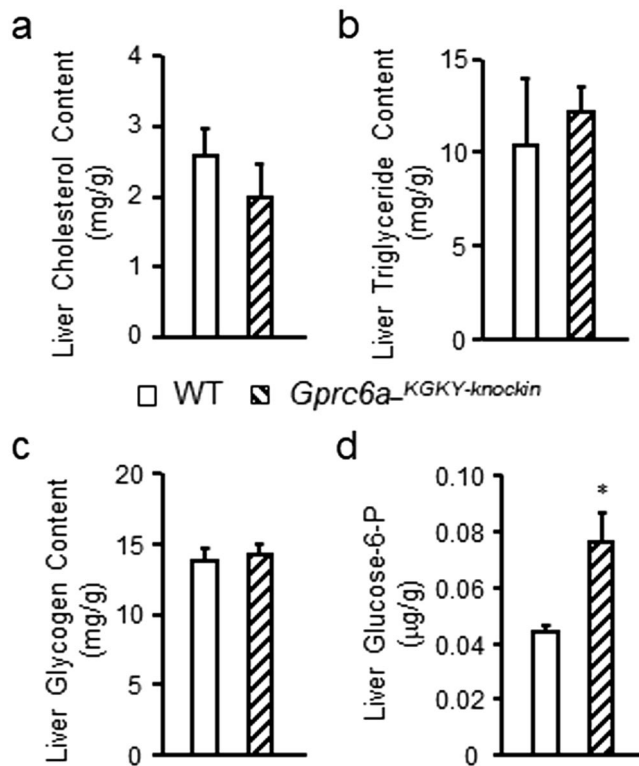


Figure 5. Characterization of additional liver parameters in *Gprc6a*^{-KGKY-knockin} mice. Comparison of the contents of cholesterol (a), triglyceride (b) and glycogen (c), and glucose-6-phosphate (Glucose-6-P) (d) in liver from control group and *Gprc6a*^{-KGKY-knockin} male mice at age of 10 week-old. Values represent the mean \pm SEM. *Significant difference between control group and *Gprc6a*^{-KGKY-knockin} mice ($P < 0.05$, Student's *t* test; $n = 6$).

Liver transcriptome in *Gprc6a*^{-KGKY-knockin} mice. Finally, we examined the liver transcriptome in *Gprc6a*^{-KGKY-knockin} mice (Fig. 6). Volcano plot (Fig. 6a) and heat map visualization (Fig. 6b) of the hepatic transcriptome demonstrated distinct differences between wild-type and *Gprc6a*^{-KGKY-knockin} mice. A total of 359 (197 upregulated and 162 downregulated) genes were identified to be differentially expressed in livers from *Gprc6a*^{-KGKY-knockin} mice and controls (adjusted $P < 0.05$) (see Table S1 for genes shown in the heat map in Fig. 6b). Biological process (GO), KEGG and mammalian phenotype enrichment analysis of the DEGs revealed that *Gprc6a*^{-KGKY-knockin} in liver resulted in differences in lipid and glucose metabolism (Fig. 6c–e). Genes induced in *Gprc6a*^{-KGKY-knockin} mice included genes involved in lipid homeostasis (6 genes), localization (20 genes), modification (7 genes), transport (14 genes), storage (10 genes), and fatty metabolic process (13 genes) (Fig. 6c). The complete list of up and down regulated genes are shown in Tables S2 and S3 in Supplemental materials.

Discussion

In the current studies, we used fine-scale genomic humanization of the GPRC6A mouse 3rd ICL to create a transgenic mouse with knock-in of the uniquely human KGKY polymorphism (*Gprc6a*^{-KGKY-knockin} mice) to determine if this polymorphism has a critical impact on the function of this G-protein coupled receptor in vivo. We found that *Gprc6a*^{-KGKY-knockin} mice differed from wild type mice expressing the ancestral RKLK variant by the presence of a lower circulating blood glucose, improved glucose tolerance test, increased serum insulin and FGF-21 concentrations. We also observed higher glucose levels in *Gprc6a*^{-KGKY-knockin} after either pyruvate or insulin administration. Thus, the GPRC6A^{-KGKY} polymorphism may enhance liver gluconeogenesis and glucose production as well as increase peripheral glucose utilization. We also observed a decrease white fat mass in *Gprc6a*^{-KGKY-knockin} mice, consistent with either direct or indirect effects of GPRC6A to regulate adipocyte function. Overall, these findings are consistent with the KGKY variant being a gain-of-function polymorphism.

Indeed, many of these phenotypic features mimic the effects of pharmacological activation of GPRC6A by Ocn treatment, which has been shown to stimulate insulin production by pancreatic β -cells, to enhance glucose and FGF-21 production by hepatocytes, to enhance glucose uptake by skeletal muscle without affecting insulin sensitivity, and to attenuate high fat diet induced hepatosteatosis in mice^{21–23,29,34–36}. A gain-of-function is also consistent with the recent in vitro findings showing that both hGPRC6A^{ICL3_KGKY} and humanized mouse mGPRC6A^{ICL3_KGKY} are retained intracellularly in ligand naive cells, but exhibit enhanced signaling responses in response to ligand stimulation^{13,32,36}.

GPRC6A is expressed in several tissues, including β -cells, skeletal muscle, adipocytes and liver^{17,29}, where it has direct effects to regulate glucose and fat metabolism. In this regard, GPRC6A is shown to have function in β -cell^{8,9,18,19}, skeletal muscle¹⁹, testes²¹, skin¹¹, adipocytes^{6,19}, and fibroblasts³⁷. Expression of the GPRC6A^{-KGKY}

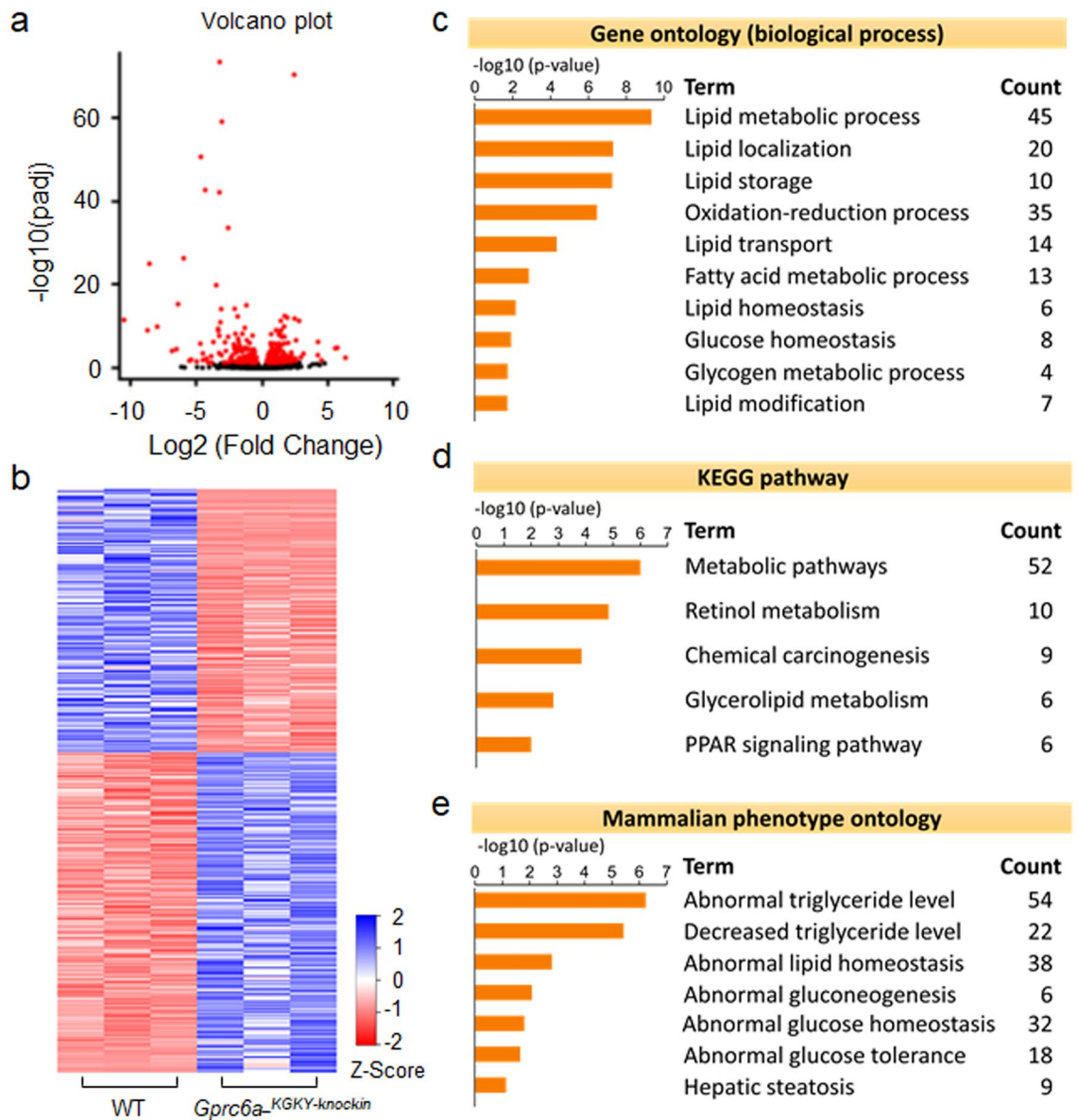


Figure 6. Hepatic gene expression in the liver of *Gprc6a*^{KGKY-knockin} mice. (A and B) Volcano plot (a); Heat map (b) of regulated genes between WT and *Gprc6a*^{KGKY-knockin} mice. Blue and red colors indicate high and low gene expression, respectively. Volcano plot and heat map visualization of the hepatic transcriptome demonstrated distinct differences between WT and *Gprc6a*^{KGKY-knockin} mice. (c–e) Gene ontology (c), the Kyoto Encyclopedia of Genes and Genomes pathway (KEGG) (d) and Mammalian phenotype ontology (e) in the liver of *Gprc6a*^{KGKY-knockin} mice. The top rank ordered processes, maps and networks are based on statistical significance.

variant in the *Gprc6a*^{KGKY-knockin} mouse under control of the endogenous promoter would be expected to express the gain-of-function polymorphism in multiple tissues. Our data suggests that GPRC6A also has important functions in the liver. Though additional studies in hepatocytes are needed, the hepatic transcriptome analysis suggests that the *GPRC6A*^{KGKY} variant may directly affect hepatic glucose metabolism by decreasing glycolysis and increasing gluconeogenesis. GPRC6A also likely regulates hepatic glycogen metabolism by increasing glycogenesis and glycogenolysis. Our findings also implicate GPRC6A in hepatic fat metabolism where the alterations in gene expression suggests an effect to decrease fatty acid uptake and fatty acid synthesis, and to increase β -oxidation. Overall, these changes on glucose and lipid metabolism in the liver are consistent with the effects of Ocn activation of GPRC6A in the liver to prevent high-fat diet induced hepatosteatosis^{17,29,36,38} and effects of Ocn to stimulate hepatic glucose production and skeletal muscle glucose uptake and utilization through GPRC6A-dependent mechanisms²².

Another mechanism whereby GPRC6A regulates systemic energy homeostasis is through the release of an ensemble of hormones, including insulin secretion in pancreatic β -cells^{3,7,9,17–19}, testosterone (T) production in Leydig cells^{2,4,21,32}, IL-6 secretion in skeletal muscle^{20,22}, adiponectin⁶ and lipocalin 2 from adipocytes³⁹ and glucagon-like peptide 1 (GLP-1) production from intestinal cells^{7,40,41}. The increased circulating levels of insulin

in *Gprc6a*^{-KGKY-knockin} are consistent with GPRC6A stimulation of insulin secretion. In addition, we show for the first time that the hormone FGF-21 is regulated by GPRC6A. We have the novel finding of elevated FGF-21 levels in *Gprc6a*^{-KGKY-knockin} mice. Moreover, treatment of wild type mice with the GPRC6A ligand Ocn resulted in increased FGF-21. Since Ocn is purported to be the cognate ligand for GPRC6A^{4-9,21}, these findings are consistent with direct hepatic effects of GPRC6A to regulate FGF-21 production. Some of the metabolic alterations in *Gprc6a*^{-KGKY-knockin} mice may be due to FGF-21. FGF-21 has paracrine effects in the liver to regulate hepatic lipid oxidation, triglyceride clearance, ketogenesis, and gluconeogenesis^{42,43}, as well as systemic effects to increase fat browning, glucose and fatty acid utilization and insulin sensitivity in muscle, to increase insulin synthesis⁴⁴, and central nervous system actions to regulate energy intake and sugar consumption³⁸. Limitations of our studies include the lack of information on the effects of dietary fat and calorie intake on the observed phenotype in *Gprc6a*^{-KGKY-knockin} mice.

The current study also addresses the controversy surrounding the function of the ICL3_KGKY polymorphism in GPRC6A in humans, which has been reported to be a hypomorphic by some investigators^{26,31}. Our findings showing a gain-of-function in *GPRC6A*^{-KGKY} mice are consistent with in vitro data showing that the endogenous human GPRC6A containing the KGKY variant in the 3rd intracellular loop is a gain-of-function polymorphism in PC-3 cells in vitro^{13,32}. The *GPRC6A*^{-KGKY} variant as a risk factor for metabolic syndrome, however, has not been well studied in human populations, and case controlled genetic associative studies have been inadequately powered to reach a definitive conclusion²⁶, although the P91S (rs2274911) SNP is associated with insulin resistance^{30,45}. Clinical association studies, however, showing that levels of Ocn, are inversely associated with glycemic status and insulin⁴⁶, body mass index, fasting glucose and insulin, triglycerides, and leptin, and positively correlated with adiponectin in humans^{33,47}, suggest that GPRC6A is functional in humans. Additional studies are needed to understand the differential functions of *GPRC6A*^{-KGKY} *GPRC6A*^{-RKLP} variants in humans. If GPRC6A is an important regulator of glucose and fat metabolism in humans, the unequally distributed RKLP and KGKY polymorphisms may impact racial differences in energy metabolism and help to explain the large variations in serum FGF-21 levels⁴⁸.

In conclusion, the emerging direct functions of GPRC6A in the liver and other tissues, its ability to coordinate the release of an ensemble of metabolically active hormones, and the ability of multiple ligands, including amino acids, cations, Ocn, T and certain natural products to activate GPRC6A, suggests activation of this G-protein coupled receptor provides a new schema for understanding and manipulating energy metabolism. Collectively, the functions of GPRC6A may be to directly and indirectly coordinate the anabolic responses of liver, muscle, fat in response to diverse hormonal and environmental factors. If so, activation of GPRC6A may provide a target to treat metabolic syndrome (MetS), type 2 diabetes (T2D), and non-alcoholic fatty liver disease (NAFLD). To this end, small molecule agonists for GPRC6A have recently been developed that lower glucose in mice⁴⁹ that may serve as therapeutic leads to develop GPRC6A agonists.

Methods

Animals. *Gprc6a*^{-KGKY-knockin} mice were generated by sgRNA/CRISPR-Cas9 target site in proximity to the RKLP → KY mutation site in The University of Alabama at Birmingham. A sgRNA targeting the site immediately preceding the RKLP region (GCTTTGTATTTCGATT-CAAG<GGG>) was selected for co-injection with Cas9 protein and a single stranded DNA oligonucleotide (ssODN-HDR; MmGprc6aHDRssODN: GGT AGTATAGACAGGGATGAATGTGATCCAAGCTATGAAGTAAATCAGCATCCCAAAGGTCAGAAGCTTG GCTTCGTTGTAATTCTCgtaTTTCCCTTAAATGCAAATACAAAGCAAATGAAGGCCAGAAGCTGTGATG TAGCCCAGCATGGTACCAAATGCCAGTGCTGACCCCTCCTCACATTCCAGGAT) repair template. The ssODN was modified to replace the mouse-specific RKLP coding sequence to the human-specific KGKY coding sequence in ICL3, and also to ensure that the modified sequence is not targeted by the CRISPR/sgRNA. PCR genotyping using MmGprc6a-gen-F2 and MmGprc6a-gen-R1 primer set. The knockin of the human *GPRC6A* KY polymorphism PCR product cut by Dra I resulted in 335 and 242 bp bands.

Mice were maintained and used in accordance with recommendations as described (National Research Council. 1985; Guide for the Care and Use of Laboratory Animals DHHS Publication NIH 86-23, Institute on Laboratory Animal Resources, Rockville, MD, USA) and following guidelines established by the University of Tennessee Health Science Center Institutional Animal Care and Use Committee. The animal study protocol was approved by the institutional review boards at University of Tennessee Health Science Center Institutional Animal Care and Use Committee.

Site-directed mutagenesis. Site-directed mutagenesis was conducted using the QuickChange mutagenesis kit (Stratagene) according to the protocols of the manufacturer using a primer set including mGPRC6A. KYfor: gattcaaggcaaatgagaattacaacgaagc and mGPRC6A.KYrev: ggcttcgtgtaattctcatattgccccttgatgc. Mutant was constructed on wild type mouse GPRC6A (mGPRC6A^{ICL3_KGRKLP} in pcDNA3 vector) background. The mGPRC6A^{ICL3_KGKY} was confirmed by DNA sequencing. HEK-293 cells were transfected with mGPRC6A^{ICL3_KGRKLP} or mGPRC6A^{ICL3_KGKY} plasmids using TransFast Transfection Reagent (Promega) for 48 h, then the transfected cells were selected by G418.

Measurement of total and phospho-ERK and -mTOR by Elisa analysis. Briefly, HEK-293 cells transfected with wild type mouse GPRC6A (mGPRC6A^{ICL3_KGRKLP}) and mGPRC6A^{ICL3_KGKY} mutant cDNA plasmids were starved by overnight incubation in serum-free DMEM/F12 containing 0.1% bovine serum albumin (BSA) and stimulated with various ligands at different doses. ERK activation were assessed the time as indicated after treatment by using ERK1/2 (phospho-T203/Y204) ELISA Kit (Invitrogen) corrected for the amount of total

ERK using ERK1/2 (Total) ELISA Kit (Invitrogen) to measure ERK levels. mTOR activation were assessed by using mTOR ELISA Kit (abcam).

Metabolic studies. The glucose tolerance test (GTT) was performed by injecting glucose (2 g/kg body weight) intraperitoneally⁵⁰ after a 5 h fast, and monitoring blood glucose using glucose strips and the Accu-Check glucometer at the indicated times⁵¹. For the insulin tolerance test³³, mice were fasted for 5 h, injected IP with insulin (0.75 U/kg body weight, Sigma; St. Louis, MO, USA), and blood glucose levels were measured at indicated times as described²⁴. For the pyruvate tolerance test (PTT), samples were collected following IP injection with pyruvate sodium (2 g/kg bodyweight) to 5 h fasted mice. Insulin (mouse) ultrasensitive ELISA kit was obtained from ALPCO Immunoassays (Salem, NH, USA). Glycogen assay and cholesterol quantitation kits were purchased from Sigma (St. Louis, MO, USA). Triglyceride colorimetric assay kit was obtained from Cayman chemical (Ann Arbor, MI, USA). Free fatty acid assay kit was purchased from Fisher Scientific (Pittsburgh, PA, USA). Rat/Mouse FGF-21 Elisa kit purchased from EMD Millipore (Burlington, MA, USA).

RNA extraction. Total RNA was extracted from mouse liver tissue (~30 mg for each sample) using QIAGEN RNeasy Mini Kit (Frederick, MD, USA). QIAGEN RNase-free DNase Set (Frederick, MD, USA) were used for RNA cleanup. RNA quantity was determined by Qubit fluorometer and RNA integrity were determined by Agilent 2100 bioanalyzer (Santa Clara, CA, USA). The qualified samples (RNA integrity number, RIN > 9) were subjected to RNA-seq analysis.

Real-time RT-PCR. We used 2.0 µg of total RNAs for reverse transcription using cDNA synthesis kit (Bio-Rad). PCR reactions were described in previously publications^{9,17}. The primers for mouse *Fgf21* (NM_020013) consisted of mFGF21-F67: CTGCTGGGGTCTACCAAG and mFGF21-R220: CTGCGCTACCACTGTTCC, and for the *Cyclophilin A* (NM_008907) consisted of *CycA*. For: CTGCACTGCCAAGACTGAAT and *CycA*. Rev: CCACAATGTTTCAT-GCCTTCT.

Library preparation and sequencing. The library preparation and sequencing were carried out by Novogene Co., Ltd. (Chula Vista, CA, USA). Briefly, mRNA was first enriched using oligo⁵² beads and fragmented randomly by adding fragmentation buffer. Then the cDNA was synthesized by using mRNA template and random hexamers primer, after which a custom second-strand synthesis buffer (Illumina; Mountain View, CA, USA), dNTPs, RNase H, and DNA polymerase I were added to initiate the second-strand synthesis. Second, after terminal repair, a ligation and sequencing adaptor ligation, the double-stranded cDNA library was completed through size selection and PCR enrichment. The library quality was accessed by Qubit 2.0, Agilent 2100, and Q-PCR. The DNA from the qualified libraries are fed into Illumina sequencers at an average depth of 42 million reads per sample.

RNA-seq data analysis. Raw reads were quality filtered with NGS QC Toolkit version 2.3⁵³ to remove adaptor contaminated reads or reads containing >20% low-quality (Q < 20) bases. Filtered reads were aligned to the mouse reference sequence (GRCm38/mm10) using STAR aligner version 2.5.0a⁵⁴. Raw read count was quantified across all annotated mm10 transcript using FeatureCounts version 1.6.3 implemented in Subread package⁵⁵, then submitted to DeSeq2 version 1.10.1⁵⁶ to identify the differentially expressed genes between *Gprc6a*^{KGKY-knockin} and WT groups (three replicates for each group). Differentially expressed genes were defined as having an adjusted P value < 0.05. Gene set enrichment analysis for Gene Ontology (GO), Kyoto Encyclopedia of Genes and Genomes (KEGG), and Mammalian Phenotype Ontology were analyzed with WebGestalt⁵⁷ (<https://www.webgestalt.org/>) with default parameters. A threshold of FDR < 0.05 was used to determine the significant enriched terms. Volcano plot and heatmaps were drawn using R program.

Statistics. We evaluated differences between groups by Student's *t* test, and for multiple groups by two-way ANOVA, followed by a post-hoc Tukey's test. Significance was set at P < 0.05. All values are expressed as means ± SEM. All computations were performed using the Statgraphic statistical graphics system (STSC Inc., Rockville, MD, USA).

Received: 5 November 2019; Accepted: 29 May 2020

Published online: 07 July 2020

References

- Pi, M. *et al.* Structural and functional evidence for testosterone activation of GPRC6A in peripheral tissues. *Mol. Endocrinol.* **29**, 1759–1773. <https://doi.org/10.1210/me.2015-1161> (2015).
- De Toni, L. *et al.* Osteocalcin and sex hormone binding globulin compete on a specific binding site of GPRC6A. *Endocrinology* **157**, 4473–4486. <https://doi.org/10.1210/en.2016-1312> (2016).
- Wei, J., Hanna, T., Suda, N., Karsenty, G. & Ducy, P. Osteocalcin promotes beta-cell proliferation during development and adulthood through Gprc6a. *Diabetes* **63**, 1021–1031. <https://doi.org/10.2337/db13-0887> (2014).
- Oury, F. *et al.* Osteocalcin regulates murine and human fertility through a pancreas-bone-testis axis. *J. Clin. Investig.* **123**, 2421–2433. <https://doi.org/10.1172/JCI65952> (2013).
- De Toni, L. *et al.* Uncarboxylated osteocalcin stimulates 25-hydroxy vitamin D production in Leydig cell line through a GPRC6a-dependent pathway. *Endocrinology* **155**, 4266–4274. <https://doi.org/10.1210/en.2014-1283> (2014).
- Otani, T. *et al.* Signaling pathway for adiponectin expression in adipocytes by osteocalcin. *Cell Signal.* **27**, 532–544. <https://doi.org/10.1016/j.cellsig.2014.12.018> (2015).

7. Mizokami, A. *et al.* Oral administration of osteocalcin improves glucose utilization by stimulating glucagon-like peptide-1 secretion. *Bone* **69**, 68–79. <https://doi.org/10.1016/j.bone.2014.09.006> (2014).
8. Pi, M., Wu, Y. & Quarles, L. D. GPRC6A mediates responses to osteocalcin in beta-cells in vitro and pancreas in vivo. *J. Bone Miner. Res.* **26**, 1680–1683. <https://doi.org/10.1002/jbmr.390> (2011).
9. Pi, M. *et al.* Evidence for osteocalcin binding and activation of GPRC6A in beta-cells. *Endocrinology* **157**, 1866–1880. <https://doi.org/10.1210/en.2015-2010> (2016).
10. Teng, B. *et al.* Newly identified peptide hormone inhibits intestinal fat absorption and improves NAFLD through its receptor GPRC6A. *J. Hepatol.* <https://doi.org/10.1016/j.jhep.2020.02.026> (2020).
11. Ko, E. *et al.* Testosterone stimulates Duox1 activity through GPRC6A in skin keratinocytes. *J. Biol. Chem.* **289**, 28835–28845. <https://doi.org/10.1074/jbc.M114.583450> (2014).
12. Pi, M., Parrill, A. L. & Quarles, L. D. GPRC6A mediates the non-genomic effects of steroids. *J. Biol. Chem.* **285**, 39953–39964. <https://doi.org/10.1074/jbc.M110.158063> (2010).
13. Ye, R., Pi, M., Nooh, M. M., Bahout, S. W. & Quarles, L. D. Human GPRC6A mediates testosterone-induced mitogen-activated protein kinases and mTORC1 signaling in prostate cancer cells. *Mol. Pharmacol.* **95**, 563–572. <https://doi.org/10.1124/mol.118.115014> (2019).
14. Pi, M. *et al.* GPCR6A is a molecular target for the natural products gallate and EGCG in green tea. *Mol. Nutr. Food Res.* **62**, e1700770. <https://doi.org/10.1002/mnfr.201700770> (2018).
15. Rueda, P. *et al.* Murine GPRC6A mediates cellular responses to L-amino acids, but not osteocalcin variants. *PLoS ONE* **11**, e0146846. <https://doi.org/10.1371/journal.pone.0146846> (2016).
16. Jacobsen, S. E. *et al.* Delineation of the GPRC6A receptor signaling pathways using a mammalian cell line stably expressing the receptor. *J. Pharmacol. Exp. Ther.* **347**, 298–309. <https://doi.org/10.1124/jpet.113.206276> (2013).
17. Pi, M. *et al.* GPRC6A null mice exhibit osteopenia, feminization and metabolic syndrome. *PLoS ONE* **3**, e3858. <https://doi.org/10.1371/journal.pone.0003858> (2008).
18. Pi, M., Wu, Y., Lenchik, N. I., Gerling, I. & Quarles, L. D. GPRC6A mediates the effects of L-arginine on insulin secretion in mouse pancreatic islets. *Endocrinology* **153**, 4608–4615. <https://doi.org/10.1210/en.2012-1301> (2012).
19. Ferron, M., Hinoi, E., Karsenty, G. & Ducy, P. Osteocalcin differentially regulates beta cell and adipocyte gene expression and affects the development of metabolic diseases in wild-type mice. *Proc. Natl. Acad. Sci. USA* **105**, 5266–5270. <https://doi.org/10.1073/pnas.071119105> (2008).
20. Mera, P., Laue, K., Wei, J., Berger, J. M. & Karsenty, G. Osteocalcin is necessary and sufficient to maintain muscle mass in older mice. *Mol. Metab.* **5**, 1042–1047. <https://doi.org/10.1016/j.molmet.2016.07.002> (2016).
21. Oury, F. *et al.* Endocrine regulation of male fertility by the skeleton. *Cell* **144**, 796–809. <https://doi.org/10.1016/j.cell.2011.02.004> (2011).
22. Mera, P. *et al.* Osteocalcin signaling in myofibers is necessary and sufficient for optimum adaptation to exercise. *Cell Metab.* **23**, 1078–1092. <https://doi.org/10.1016/j.cmet.2016.05.004> (2016).
23. Karsenty, G. & Olson, E. N. Bone and muscle endocrine functions: unexpected paradigms of inter-organ communication. *Cell* **164**, 1248–1256. <https://doi.org/10.1016/j.cell.2016.02.043> (2016).
24. Lee, N. K. *et al.* Endocrine regulation of energy metabolism by the skeleton. *Cell* **130**, 456–469. <https://doi.org/10.1016/j.cell.2007.05.047> (2007).
25. Jorgensen, C. V. *et al.* Metabolic and skeletal homeostasis are maintained in full locus GPRC6A knockout mice. *Sci. Rep.* **9**, 5995. <https://doi.org/10.1038/s41598-019-41921-8> (2019).
26. Jorgensen, S. *et al.* Genetic variations in the human G protein-coupled receptor Class C, Group 6, Member A (GPRC6A) control cell surface expression and function. *J. Biol. Chem.* **292**, 1524–1534. <https://doi.org/10.1074/jbc.M116.756577> (2017).
27. Lambert, L. J. *et al.* Increased trabecular bone and improved biomechanics in an osteocalcin-null rat model created by CRISPR/Cas9 technology. *Dis. Models Mech.* **9**, 1169–1179. <https://doi.org/10.1242/dmm.025247> (2016).
28. Pi, M. *et al.* Identification of a novel extracellular cation-sensing G-protein-coupled receptor. *J. Biol. Chem.* **280**, 40201–40209. <https://doi.org/10.1074/jbc.M505186200> (2005).
29. Pi, M., Nishimoto, S. K. & Quarles, L. D. GPRC6A: jack of all metabolism (or master of none). *Mol. Metab.* **6**, 185–193. <https://doi.org/10.1016/j.molmet.2016.12.006> (2017).
30. Di Nisio, A. *et al.* The rs2274911 polymorphism in GPRC6A gene is associated with insulin resistance in normal weight and obese subjects. *Clin. Endocrinol.* <https://doi.org/10.1111/cen.13248> (2016).
31. Jacobsen, S. E. *et al.* The GPRC6A receptor displays constitutive internalization and sorting to the slow recycling pathway. *J. Biol. Chem.* **292**, 6910–6926. <https://doi.org/10.1074/jbc.M116.762385> (2017).
32. Ye, R., Pi, M., Cox, J. V., Nishimoto, S. K. & Quarles, L. D. CRISPR/Cas9 targeting of GPRC6A suppresses prostate cancer tumorigenesis in a human xenograft model. *J. Exp. Clin. Cancer Res. CR* **36**, 90. <https://doi.org/10.1186/s13046-017-0561-x> (2017).
33. Pittas, A. G., Harris, S. S., Eliades, M., Stark, P. & Dawson-Hughes, B. Association between serum osteocalcin and markers of metabolic phenotype. *J. Clin. Endocrinol. Metab.* **94**, 827–832. <https://doi.org/10.1210/jc.2008-1422> (2009).
34. Ferron, M. *et al.* Insulin signaling in osteoblasts integrates bone remodeling and energy metabolism. *Cell* **142**, 296–308. <https://doi.org/10.1016/j.cell.2010.06.003> (2010).
35. Du, J. *et al.* Osteocalcin improves nonalcoholic fatty liver disease in mice through activation of Nrf2 and inhibition of JNK. *Endocrine* **53**, 701–709. <https://doi.org/10.1007/s12020-016-0926-5> (2016).
36. Gupte, A. A. *et al.* Osteocalcin protects against nonalcoholic steatohepatitis in a mouse model of metabolic syndrome. *Endocrinology* **155**, 4697–4705. <https://doi.org/10.1210/en.2014-1430> (2014).
37. Fujiwara, T. *et al.* L-Arginine stimulates fibroblast proliferation through the GPRC6A-ERK1/2 and PI3K/Akt pathway. *PLoS ONE* **9**, e92168. <https://doi.org/10.1371/journal.pone.0092168> (2014).
38. Gillum, M. P. Parsing the potential neuroendocrine actions of FGF21 in primates. *Endocrinology* **159**, 1966–1970. <https://doi.org/10.1210/en.2018-00208> (2018).
39. Mosialou, I. *et al.* MC4R-dependent suppression of appetite by bone-derived lipocalin 2. *Nature* **543**, 385–390. <https://doi.org/10.1038/nature21697> (2017).
40. Mizokami, A. *et al.* Osteocalcin induces release of glucagon-like peptide-1 and thereby stimulates insulin secretion in mice. *PLoS ONE* **8**, e57375. <https://doi.org/10.1371/journal.pone.0057375> (2013).
41. Oya, M. *et al.* The G protein-coupled receptor family C group 6 subtype A (GPRC6A) receptor is involved in amino acid-induced glucagon-like peptide-1 secretion from GLUTag cells. *J. Biol. Chem.* **288**, 4513–4521. <https://doi.org/10.1074/jbc.M112.402677> (2013).
42. Badman, M. K., Koester, A., Flier, J. S., Kharitonov, A. & Maratos-Flier, E. Fibroblast growth factor 21-deficient mice demonstrate impaired adaptation to ketosis. *Endocrinology* **150**, 4931–4940. <https://doi.org/10.1210/en.2009-0532> (2009).
43. Badman, M. K. *et al.* Hepatic fibroblast growth factor 21 is regulated by PPARα and is a key mediator of hepatic lipid metabolism in ketotic states. *Cell Metab.* **5**, 426–437 (2007).
44. Inagaki, T. Research Perspectives On The Regulation And Physiological Functions of FGF21 and its association with NAFLD. *Front. Endocrinol.* **6**, 147. <https://doi.org/10.3389/fendo.2015.00147> (2015).
45. De Toni, L. *et al.* Polymorphism rs2274911 of GPRC6A as a novel risk factor for testis failure. *J. Clin. Endocrinol. Metab.* **101**, 953–961. <https://doi.org/10.1210/jc.2015-3967> (2016).

46. Iki, M. *et al.* Serum undercarboxylated osteocalcin levels are inversely associated with glycemic status and insulin resistance in an elderly Japanese male population: Fujiwara-kyo Osteoporosis Risk in Men (FORMEN) Study. *Osteoporos. Int.* <https://doi.org/10.1007/s00198-011-1600-7> (2011).
47. Foresta, C. *et al.* Androgens modulate osteocalcin release by human visceral adipose tissue. *Clin. Endocrinol.* <https://doi.org/10.1111/j.1365-2265.2011.03997.x> (2011).
48. Galman, C. *et al.* The circulating metabolic regulator FGF21 is induced by prolonged fasting and PPARalpha activation in man. *Cell Metab.* **8**, 169–174. <https://doi.org/10.1016/j.cmet.2008.06.014> (2008).
49. Pi, M. *et al.* Computationally identified novel agonists for GPRC6A. *PLoS ONE* **13**, e0195980. <https://doi.org/10.1371/journal.pone.0195980> (2018).
50. Echeverri, C. J. *et al.* Minimizing the risk of reporting false positives in large-scale RNAi screens. *Nat. Methods* **3**, 777–779. <https://doi.org/10.1038/nmeth1006-777> (2006).
51. Phillips, C. M. *et al.* Leptin receptor polymorphisms interact with polyunsaturated fatty acids to augment risk of insulin resistance and metabolic syndrome in adults. *J. Nutr.* **140**, 238–244. <https://doi.org/10.3945/jn.109.115329> (2010).
52. Taylor, C. R., Schmidt-Nielsen, K. & Raab, J. L. Scaling of energetic cost of running to body size in mammals. *Am. J. Physiol.* **219**, 1104–1107 (1970).
53. Patel, R. K. & Jain, M. NGS QC Toolkit: a toolkit for quality control of next generation sequencing data. *PLoS ONE* **7**, e30619 (2012).
54. Dobin, A. *et al.* STAR: ultrafast universal RNA-seq aligner. *Bioinformatics* **29**, 15–21 (2013).
55. Liao, Y., Smyth, G. K. & Shi, W. featureCounts: an efficient general purpose program for assigning sequence reads to genomic features. *Bioinformatics* **30**, 923–930 (2013).
56. Love, M. I., Huber, W. & Anders, S. Moderated estimation of fold change and dispersion for RNA-seq data with DESeq2. *Genome Biol.* **15**, 550 (2014).
57. Liao, Y., Wang, J., Jaehnig, E. J., Shi, Z. & Zhang, B. WebGestalt 2019: gene set analysis toolkit with revamped UIs and APIs. *Nucleic Acids Res.* **47**, 199–205 (2019).

Acknowledgements

This work was supported by grants from NIH grant R01 AR37308 and ADA grant 1-13-BS-149-BR (to LDQ), and NIH grant R01 DK120567 (to LDQ and LL). The authors would like to thank members of the University of Alabama at Birmingham Transgenic and Genetically Engineered Models (TGEMS) facility for creating the *Gprc6a* knockin animals. TGEMS is supported by NIH National Cancer Institute Grant P30CA13148, NIH National Institute of Arthritis and Musculoskeletal and Skin Diseases Grant P30AR048311, and NIH NIDDK Grants P30 DK074038, P30 DK05336, and P60 DK079626 (to RAK).

Author contributions

M.P., F.X., L.L. and L.D.Q. contributed to study design. M.P., F.X., S.K.N., L.L. and L.D.Q. wrote the manuscript with input from all authors and contributed discussion and data analysis. M.P. and R.Y. performed all experiments related to mouse phenotypic characterization and RNA sample preparation. F.X., L.L., and R.W.W. contributed to bioinformatics analysis. R.A.K. generated the *Gprc6a*^{KGKY-knockin} mice.

Competing interests

The authors declare no competing interests.

Additional information

Supplementary information is available for this paper at <https://doi.org/10.1038/s41598-020-68113-z>.

Correspondence and requests for materials should be addressed to M.P. or L.D.Q.

Reprints and permissions information is available at www.nature.com/reprints.

Publisher's note Springer Nature remains neutral with regard to jurisdictional claims in published maps and institutional affiliations.



Open Access This article is licensed under a Creative Commons Attribution 4.0 International License, which permits use, sharing, adaptation, distribution and reproduction in any medium or format, as long as you give appropriate credit to the original author(s) and the source, provide a link to the Creative Commons license, and indicate if changes were made. The images or other third party material in this article are included in the article's Creative Commons license, unless indicated otherwise in a credit line to the material. If material is not included in the article's Creative Commons license and your intended use is not permitted by statutory regulation or exceeds the permitted use, you will need to obtain permission directly from the copyright holder. To view a copy of this license, visit <http://creativecommons.org/licenses/by/4.0/>.

© The Author(s) 2020